Synthesis and Characterization of blue light excitable red emitting $Ca_4SiAl_3N_7:Eu^{2+}$ phosphor

Monika Khale* and Sudeshna Ray

Advanced Materials Research Centre, Faculty of Science

Rabindranath Tagore University, Bhopal, India

Abstract: In this work, we elucidate the synthesis and characterization and photoluminescence study of a blue light excitable red emitting $Ca_4SiAl_3N_7:Eu^{2+}$ phosphor. The phosphors were developed by an 'amorphous based metal complex method' using a water soluble silicon compound. The phase purity of the phosphors has been verified by X-ray powder diffraction technique. The sizes of the phosphor particles are measured by capturing SEM images. The phosphor exhibits a broad excitation spectrum in visible region and a broad red emission band under the visible excitation. High Temperature Photoluminescence Spectra has also been measured which evidences that the phosphor is thermally stable. The developed red-emitting phosphor shows immense potential for integration of it into the phosphor-converted LED devices for indoor farming applications.

1. Introduction:

White light-emitting diodes (WLEDs) have supplanted conventional lighting techniques as a new generation of lighting technology. Their high efficiency, stability, and environmental protection have contributed to them popular in an array of applications, including indoor lighting and medical treatment [1]. Presently available WLEDs employ a blue chip to excite yellow phosphor to generate white light; however, this scheme is devoid of a red component and has a low color rendering index (CRI < 80) and a high correlated color temperature (CCT > 4500 K), both of which are detrimental to reducing eye fatigue in humans [2], [3], [4].

In order to further improve the luminous efficiency and stability of phosphors and achieve more effective, energy-efficient, and ecologically friendly white luminescence, it is imperative to create novel red phosphors that can be efficiently activated by near-ultraviolet and blue light. This offers enormous development potential and will greatly enhance WLED performance and application value.

On the other hand, the application of LED technology in the field of indoor plant cultivation is gradually gaining widespread attention because of its ability to promote plant growth as well as its low power consumption, which can save costs and resources [5]. Light has the most significant effect on plant growth among the influencing

variables. Chlorophyll, carotenoids, and photosensitive pigments PR/PFR are the primary regulators of photosynthesis in plants. The absorption spectra of chlorophyll A/B, which predominates in photosynthesis, are concentrated in the red (580–680 nm) and blue (350–480 nm) areas, respectively [6], [7], [8]. Therefore, in order to maximize plant growth in the domain of plant farming, it is essential to design unique light conditions that particularly satisfy these spectrum requirements. Many researchers have utilized the deep red light emitted at about 690 nm by the $^2E_G \rightarrow {}^4A_2$ g jump of Mn^{4+} ions to satisfy the red-light requirement for plant growth, e.g., $Ca_2LaSbO_6:Mn^{4+}$, $CaGdMgNbO_6:Mn^{4+}$, $Li_2MgZrO_4:Mn^{4+}$, etc. [9], [10], [11].

However, Mn^{4+} ions limit their practical application in indoor plant cultivation due to their forbidden leaps resulting in weak emission intensity. The spectral absorption of chlorophyll and the photosynthetic pigment PR is limited, despite the fact that the deep red emission of Eu^{3+} ions near 708 nm (caused by the $^5D_0 \rightarrow {}^7F_4$ leaps) matches the absorption of the photosynthetic pigment PFR, which is advantageous for plant growth [12], [13], [14]. Moreover, the simultaneous use of commercially available blue and red LED chips with narrow-band emission limits their effectiveness, whereas the use of blue LEDs to excite red phosphors precisely overcomes this limitation and improves photosynthetic yield [15], [16]. Therefore, the discovery of an effective red luminous material that may be aroused with blue chips to foster plant growth is of vital importance.

Eu^{2+} possesses a unique 4*f*-5d electron jump that makes its emission energy vary in the UV and deep red spectral range [17]. For example, as $Rb_3Y(PO_4)_2:Eu^{2+}$ (λ_{em} = 426 nm) [18], $K_2BaCa(PO_4)_2:Eu^{2+}$ (λ_{em} = 460 nm) [19], $Ba_3YAl_2O_{7.5}:Eu^{2+}$ (λ_{em} = 550 nm) [20], $CaLuGaO_4:Eu^{2+}$ (λem = 650 nm) [21], $Ca_3Sc_2Si_3O_{12}:Eu^{2+}$ (λ_{em} = 876 nm) [22]. The emission spectrum of the rare earth ion Eu^{2+} generally depends on the type of ligand ion to which it is coordinated [23], [24]. Therefore, Eu^{2+}-doped phosphors are capable of achieving variable luminescence output, which effectively meets the needs of diverse applications [25].

To satisfy WLED applications and plant growth conditions, we prefer to obtain red phosphors. In recent years, some Eu^{2+}-doped sulfide- and nitride-based red phosphors possessing properties such as tunable crystal structure and efficient luminescence have gradually attracted attention. However, their practical applications are greatly limited by many factors such as easy chemical degradation, high preparation cost, and spectral overlap with YAG: Ce^{3+} [26]. In contrast, Eu2+-doped oxide phosphor is a competitive phosphor with better chemical stability, lower cost, and lower spectral reabsorption effect [27].

In this paper, we report the successful synthesis of the nitride-alumosilicate red phosphor $Ca_4SiAl_3N_7:Eu^{2+}$ at normal pressure and lower temperature (1300 °C). Under excitation with 460 nm blue light, the $Ca_4SiAl_3N_7:Eu^{2+}$ phosphor efficiently emits red light at 645 nm and exhibits excellent thermal stability. The crystal structure and luminescence properties of $Ca_4SiAl_3N_7:Eu^{2+}$ were investigated in detail. The results indicate that $Ca_4SiAl_3N_7:Eu^{2+}$ exhibits strong potential its use for the fabrication of phosphor-converted-LEDs.

2. Materials and Methods

$Ca_4SiAl_3N_7:Eu^{2+}$ phosphor was prepared through the Amorphous Metal Complex (AMC) route employing a water-soluble silicon precursor. In a representative procedure, aluminum nitrate nonahydrate [$Al(NO_3)_3 \cdot 9H_2O$, Sigma Aldrich, 99%] and calcium carbonate ($CaCO_3$, Merck, 98%) were dissolved in a citric acid medium along with europium nitrate [$Eu(NO_3)_3$, Sigma Aldrich, 99.9%]. Propylene glycol modified silane (PGMS) served as the silicon source. PGMS was synthesized via an acid-catalyzed alkoxy exchange reaction between propylene glycol (PG, Rankem, 99%) and tetraethyl orthosilicate (TEOS, Sigma Aldrich, 98%).

For the preparation of PGMS, 0.4 mol of PG and 0.1 mol of TEOS were introduced into a 100 mL stoppered conical flask using a digital pipette. Because TEOS is immiscible with PG, the initial mixture separated into two liquid layers. To promote the alkoxy exchange process, 1 mL of concentrated hydrochloric acid (HCl) was added as a catalyst. The reaction mixture was magnetically stirred at 80 °C for 1 hour, yielding a clear and homogeneous solution with no visible phase separation. The resulting product was fully miscible with water in any proportion without undergoing hydrolysis, and this modified silane precursor was designated as PGMS. The solution was then transferred to a 100 mL volumetric flask and diluted with distilled water to prepare a 1 M PGMS solution.

The target composition was fixed at a molar ratio of Ca:Eu:PGMS:Al = 4:0.04:1:3. In the AMC synthesis, stoichiometric quantities of aluminum nitrate, calcium carbonate, and europium nitrate were first dissolved in citric acid solution and stirred at 80 °C for 2 hours to form a uniform mixture. Subsequently, the temperature was increased to 130 °C, and the calculated amount of PGMS was introduced. Continued heating led to complete solvent evaporation and the formation of a transparent gel.

The obtained gel was subjected to sequential heat treatments: initially at 450 °C for 12 hours, followed by calcination at 550 °C for 4 hours in air, and finally heated at 800 °C for 5 hours to produce the precursor powder. The precursor was finely ground using an agate mortar and pestle. Nitridation was then carried out at 1300 °C for 1–9 hours under a continuous flow of ammonia gas (50 mL/min) to obtain the desired oxynitride phosphor. A schematic illustration of the overall synthesis process is shown in Fig. 1.

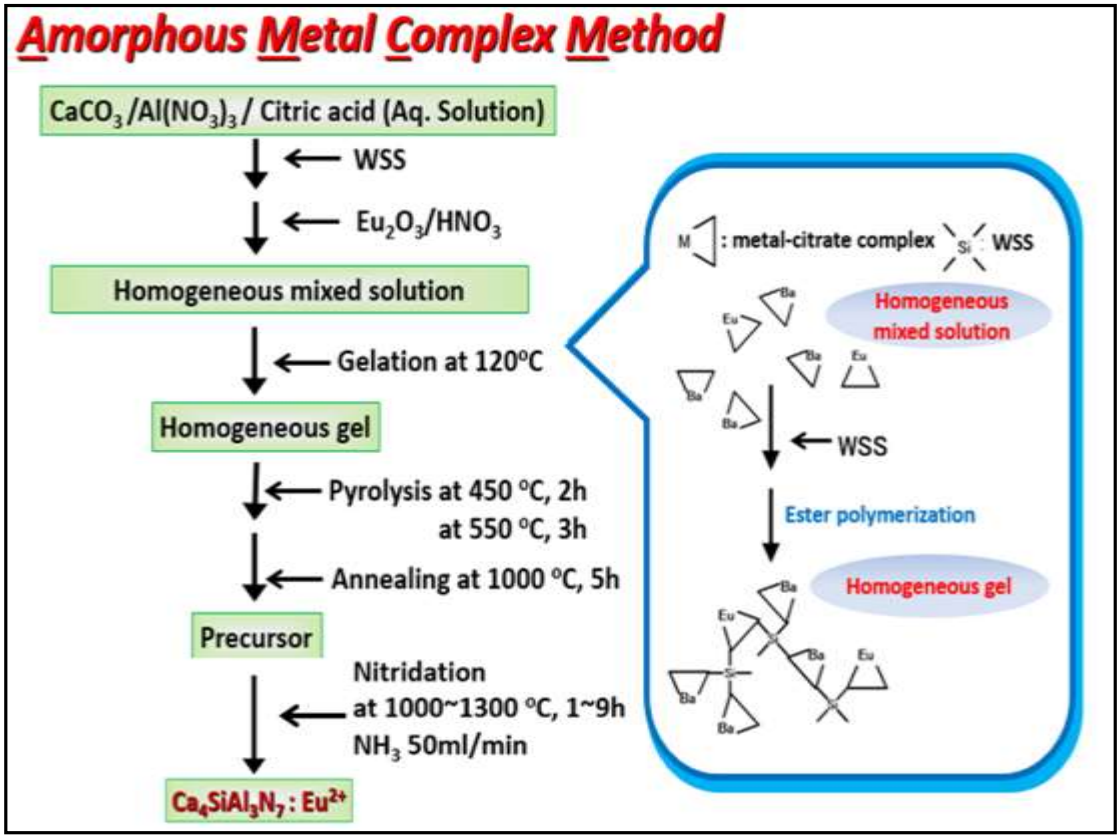

Fig. 1 Schematic representation of 'Amorphous Metal Complex' based synthesis of $Ca_4SiAl_3N_7$ doped Eu^{2+} phosphor

3. Results and discussion

3.1 Phase analysis

The XRD patterns of $Ca_4SiAl_3N_7:Eu^{2+}$(1%) are shown in Fig. 2. All the diffraction peaks were identified as crystalline $Ca_4SiAl_3N_7$ phase (ICSD-161796) indicating that a single-phased $Ca_4SiAl_3N_7$was successfully synthesized and the phase was present in the crystal lattice in high purity.

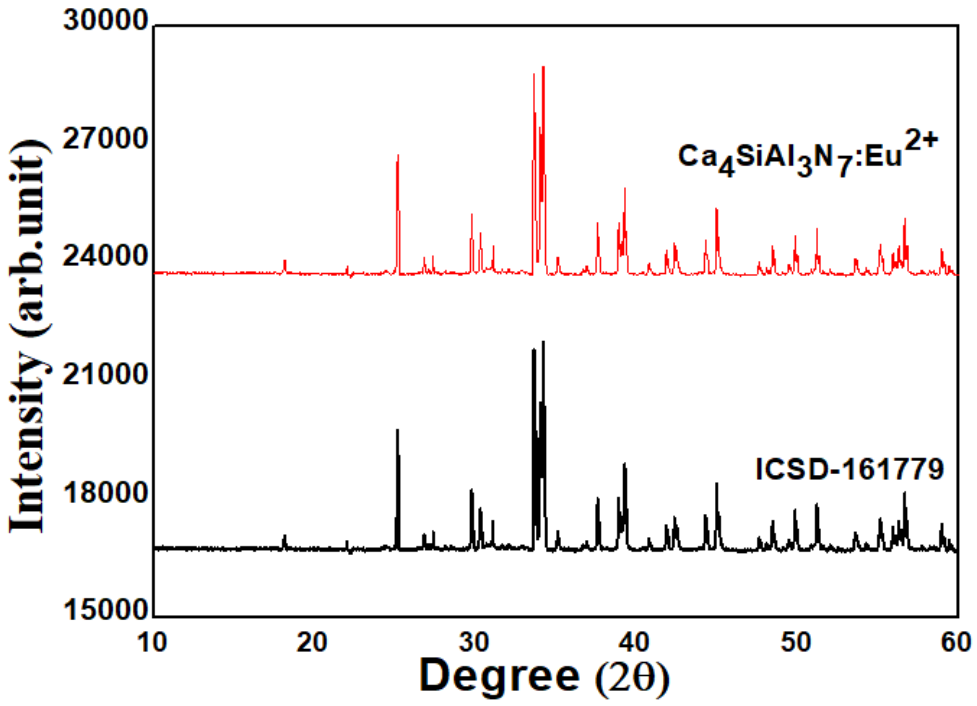

Fig. 2 XRD patterns of $Ca_4SiAl_3N_7$ doped Eu^{2+} phosphor

3.2 Crystal structure

$Ca_4SiAl_3N_7$ crystallize with three-dimensional network structures shown in Fig. 3, $Ca_4SiAl_3N_7$ belongs to triclinic system with the space group of P−1(2). SiN_4 tetrahedra and AlN_4 tetrahedra are connected to each other by common vertexes and edges to form the $Ca_4SiAl_3N_7$ framework, where the common edge connection only exists between the AlN_4 tetrahedra. The common edge connection of AlN_4 is conducive to enhancing the lattice rigidity, which is very common in nitride-alumosilicate, such as $Ca_5Si_2Al_2N_8$ and $SrAlSi_4N_7$. Ca atoms occupy tetrahedral cavities to ensure the electrical neutrality of the lattice. There are six types of Ca atoms in the lattice and all Ca atoms form distorted octahedra with adjacent N atoms. The Ca–N bond lengths range from 2.3462 Å to 3.0645 Å with the average bond length of 2.6231 Å, which is comparable to that of $Ca_5Si_2Al_2N_8$ (2.684 Å) and $CaAlSiN_3$ (2.637 Å). In anionic network structure of $Ca_4SiAl_3N_7$ is closed AlN_4 tetrahedra (dark green), mixed $SiAlN_4$ tetrahedra (light green), SiN_4 tetrahedra (yellow), Ca^{2+} cations (blue balls).

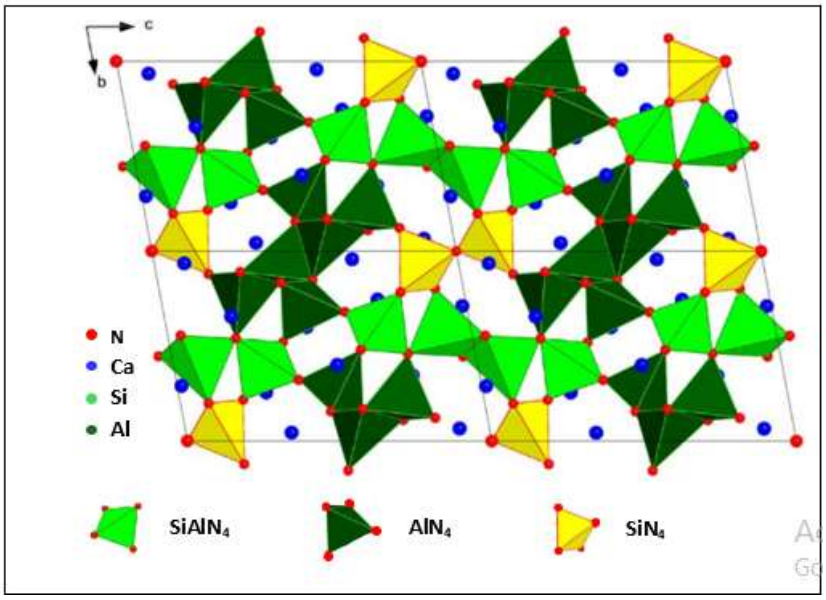

Fig. 3. Crystal Structure of $Ca_4SiAl_3N_7$ host

Fig. 4 Shows the SEM image of the $Ca_4SiAl_3N_7$ sample. The particles show irregular shape, good dispersion and smooth surface. The particles-like grains with a preferred orientation can be observed.

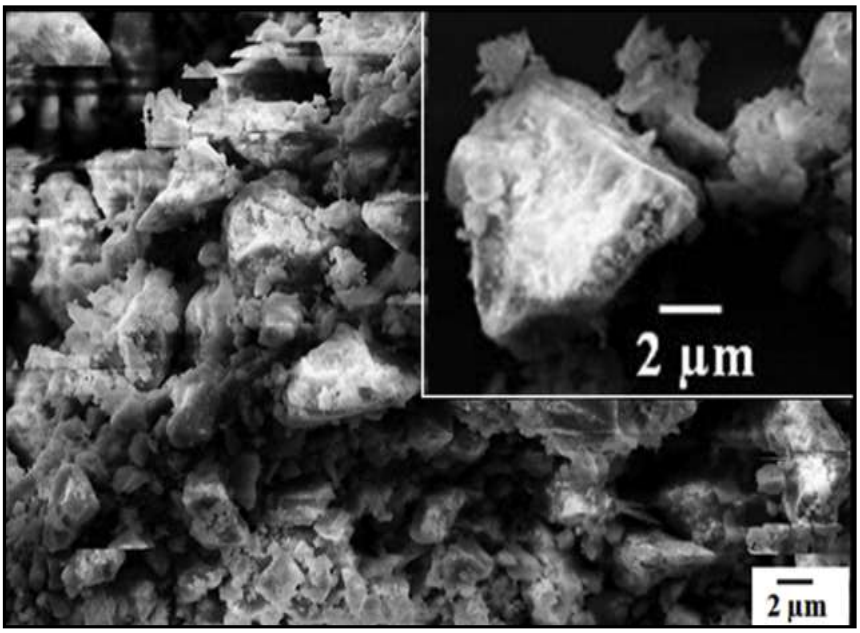

Fig. 4 SEM image of $Ca_4SiAl_3N_7$: (1%) Eu^{2+} phosphor

4. Photoluminescence properties

Fig. 5(a) shows The excitation spectrum and the corresponding emission spectrum of the sample of $Ca_4SiAl_3N_7:Eu^{2+}$ when monitored at 655 nm and excited at 460 nm, respectively. The excitation spectrum of

$Ca_4SiAl_3N_7:Eu^{2+}$ consists of various broad peaks, which are distributed over 350–550 nm. The strongest peak is at 460 nm, indicating that $Ca_4SiAl_3N_7:Eu^{2+}$ could be efficiently excited by blue LED chip [28].

The red photoluminescence (PL) of $Ca_4SiAl_3N_7:Eu^{2+}$ utilized in w-LEDs is mainly because of the 4*f*-5d excitation in the region of 350-550 nm shown in Fig. 5 (a). The room-temperature PL spectra of $Ca_4SiAl_3N_7:Eu^{2+}$ are given in Fig. 5(b). Under excitation at 460 nm, emission spectrum exhibits a broadband red emission with a full width at half maximum (FWHM) of 140 nm (4.02×10^3 cm^{-1}) and the strongest peak is at 568 nm, which is attributed to the 5d-4*f* transition of Eu^{2+}.

Fig. 5 Photoluminescence spectra of $Ca_4SiAl_3N_7$: Eu^{2+} (a) Excitation spectra at λ_{em} – 655 nm (b) Emission spectra of at λ_{ex} – 460 nm

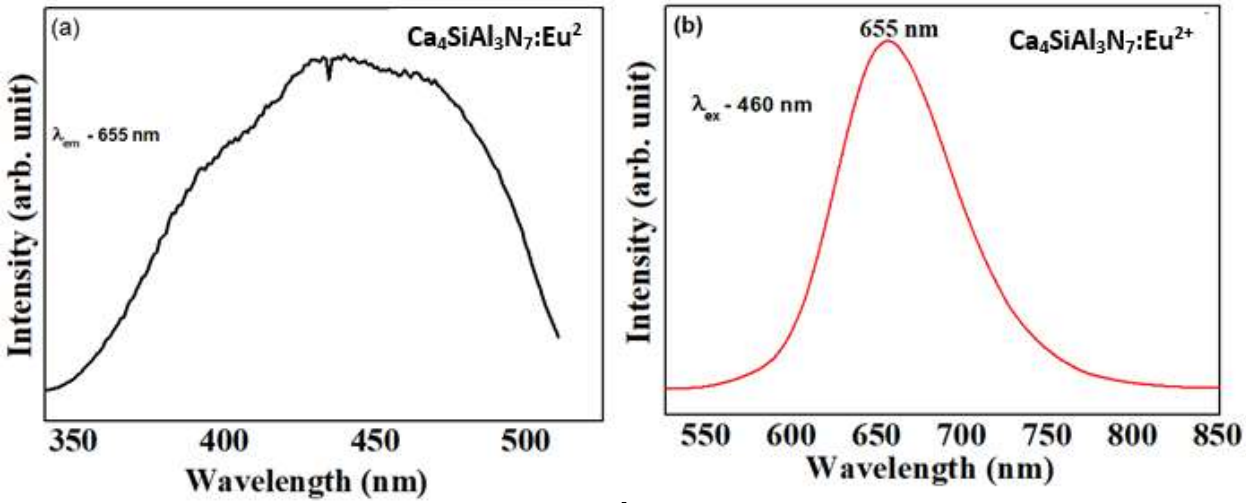

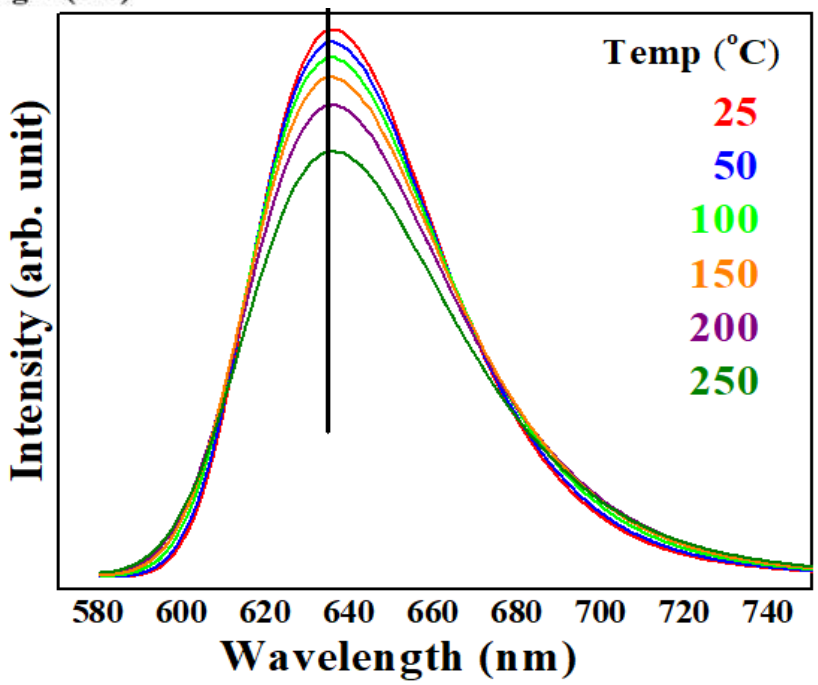

Fig. 6 Temperature dependent PL Spectra of $Ca_4SiAl_3N_7:Eu^{2+}$

Fig. 6 shows the temperature-dependent spectra of emission $Ca_4SiAl_3N_7:Eu^{2+}$. It has been identified that $Ca_4SiAl_3N_7:Eu^{2+}$ phosphor shows a low thermal quenching. Although the emission intensity gradually declines as the temperature increases, the phosphor can still retain 75% and 68% of the strength at room temperature PL intensity at 150°C and 250°C, respectively. Furthermore, except for the increase of FWHM, the emission position of the peak did not shift. These results substantiate the suitability of the as-synthesized phosphor for the fabrication of phosphor-converted LEDs.

The Commission Internationale de l'Éclairage (CIE) chromaticity coordinates of the $Ca_4SiAl_3N_7:Eu^{2+}$ phosphor under 460 nm excitation were mapped onto the CIE 1931 chromaticity diagram, as illustrated in Fig. 7. The calculated color coordinates were determined to be (x, y) = (0.654, 0.365). These values clearly confirm that the phosphor exhibits red light emission.

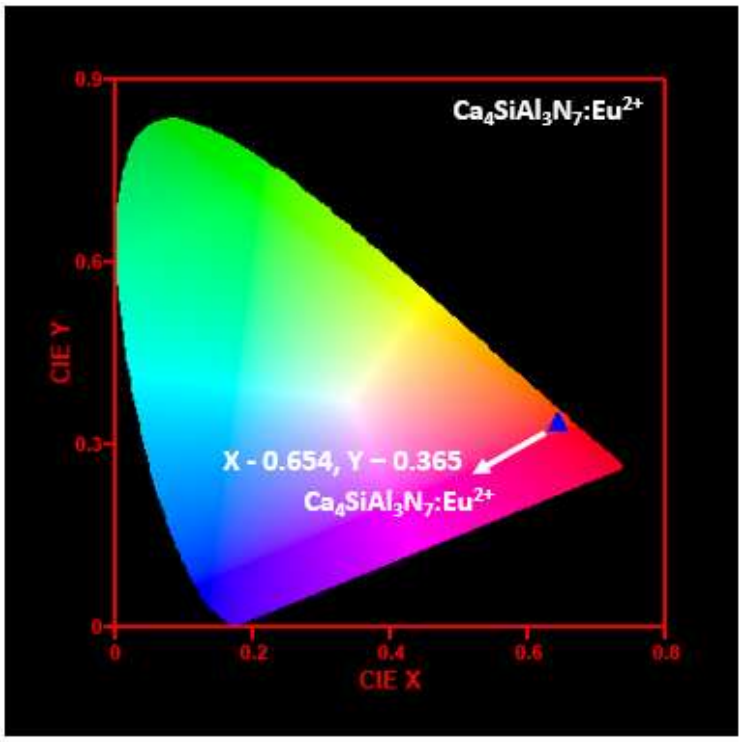

Fig. 7 CIE coordinates of $Ca_4SiAl_3N_7:Eu^{2+}$ phosphor

5. Conclusion:

In summary, blue light excitable red emitting $Ca_4SiAl_3N_7:Eu^{2+}$ phosphor was synthesized by an ‘amorphous metal based The complexation technique employs a water-soluble silicon precursor as the primary source material for the synthesis process as silicon precursor. The phosphor was characterized through XRD and SEM. Photoluminescence ‘Excitation’, ‘Emission’ and ‘High Temperature Photoluminescence Spectra’ have been

measured. The results of all these measurements substantiate The prepared red-emitting phosphor, which can be efficiently excited by blue light, demonstrates strong suitability for incorporation into phosphor-converted LED.

6. References:

[1] S. Nakamura, G. Fasol, The Blue Laser Diode: GaN Based Light Emitters and Lasers, Springer, Berlin, 1997.

[2] N. Hirosaki, R.J. Xie, K. Kimoto, T. Sekiguchi, Y. Yamamoto, T. Suehiro, M. Mitomo, Appl. Phys. Lett. 86 (2005) 211905.

[3] H. Huppertz, W. Schnick, Z. Anorg. Allg. Chem. 623 (1997) 212.

[4] R.J. Xie, N. Hirosaki, H.L. Li, Y.Q. Li, M. Mitomo, J. Electrochem. Soc. 154 (2007) J314.

[5] R.J. Xie, N. Hirosaki, M. Mitomo, K. Uheda, T. Suehiro, Y. Xu, Y. Yamamoto, T. Sekiguchi, J. Phys. Chem. B 109 (2005) 9490.

[6] Y.Q. Li, A.C.A. Delsing, G. de With, H.T. Hintzen, Chem. Mater. 17 (2005) 3242.

[7] Y.Q. Li, C.M. Fang, G. de With, H.T. Hintzen, J. Solid State Chem. 177 (2004) 4687.

[8] F.C. Palilla, B.E. O'Reilly, V.J. Abbruscato, J. Electrochem. Soc. 117 (1970) 87.

[9] O.J. Rubio, J. Phys. Chem. Solids 521 (1991) 101.

[10] S. Lizzo, A. Meijerink, G. Blasse, J. Lumin. 59 (1994) 185.

[11] J.W.H. van Krevel, J.W.T. Rutten, H. Mandal, H.T. Hinzen, R. Metselaar, J. Solid State Chem. 165 (2002) 19.

[12] X.F. Song, H. He, R.L. Fu, D.L. Wang, X.R. Zhao, Z.W. Pan, J. Phys. D: Appl. Phys. 42 (2009) 065409.

[13] K. Uheda, N. Hirosaki, Y. Yamamoto, A. Naito, T. Nakajima, H. Yamamoto, Electrochem. Solid State Lett. 9 (2006) H22.

[14] H. Watanabe, N. Kijima, J. Alloys Comp. 475 (2009) 434.

[15] H.A. Höppe, H. Lutz, P. Morys, W. Schnick, A. Seilmeier, J. Phys. Chem. Solids 61 (2000) 2001.

[16] X. Piao, K. Machida, T. Horikawa, H. Hanzawa, Y. Shimomura, N. Kijima, Chem. Mater. 19 (2007) 4592.

[17] N. Hirosaki, K. Uheda, Japanese Patent, 2005, P2005-336253A.

[18] K.M. Sparta, R. Mueller, M. Merz, G. Roth, P. Adelmann, T. Wolf, Acta Cryst. B 62 (2006) 710.

[19] M. Imai, K. Nishida, T. Kimura, H. Abe, Appl. Phys. Lett. 80 (2002) 1019.

[20] D. Kuramoto, H.-S. Kim, T. Horikawa, M. Itoh, K. Machida, J. Phys: Conf. Ser. 379 (2012) 012015.

[21] A.G. Merzhanov, A.S. Rogachev, Pure Appl. Chem. 64 (1992) 941.

[22] A. Boultif, D. Louer, J. Appl. Crystallogr. 37 (2004) 724.

[23] J. Rodr´ıguez-Carvajal, Physica B 192 (1993) 55.

[24] T. Roisnel, J. Rodr´ıguez-Carvajal, Mater. Sci. Forum 118–123 (2001) 378.

[25] J. Li, T. Watanabe, H. Wada, T. Setoyama, M. Yoshimura, Chem. Mater. 19 (2007) 3592–3594.

[26] J. Li, T. Watanabe, N. Sakamoto, H. Wada, T. Setoyama, M. Yoshimura, Chem. Mater. 20 (2008) 2095–2105.

[27] B. Dierre, T. Takeda, T. Sekiguchi, T. Suehiro, K. Takahashi, Y. Yamamoto, R.J. Xie, N. Hirosaki, Sci. Technol. Adv. Mater. 14 (2013) 064201.

[28] H.S. Kim, K. Machida, T. Horikawa, H. Hanzawa, Chem. Lett. 43 (2014) 533– 534.